Appl Phys B (2009) 94: 375–379
DOI 10.1007/s00340-008-3347-1

Applied Physics B
Lasers and Optics

Mode-locked diode-pumped vanadate lasers operated with PbS quantum dots

A.A. Sirotkin · L. Di Labio · A.I. Zagumennyi · Yu.D. Zavartsev · S.A. Kutovoi · V.I. Vlasov · W. Lüthy · T. Feurer · A.A. Onushchenko · I.A. Shcherbakov

Received: 15 July 2008 / Revised version: 29 October 2008 / Published online: 10 January 2009

Abstract The use of glasses doped with PbS nanocrystals as intracavity saturable absorbers for passive Q-switching and mode locking of c-cut $Nd{:}Gd_{0.7}Y_{0.3}VO_4$, $Nd{:}YVO_4$, and $Nd{:}GdVO_4$ lasers is investigated. Q-switching yields pulses as short as 35 ns with an average output power of 435 mW at a repetition rate of 6–12 kHz at a pump power of 5–6 W. Mode locking through a combination of PbS nanocrystals and a Kerr lens results in 1.4 ps long pulses with an average output power of 255 mW at a repetition rate of 100 MHz.

PACS 42.55.Xi · 42.60.Fc · 42.70.Hj

1 Introduction

Generating stable short pulses in the infrared spectral range from diode-pumped lasers is still an active area of research. Nano-, pico- and femtosecond laser pulses find applications in telecommunication, biology, medicine, chemistry, and material processing. Passive modulators for mode locking and Q-switching are very favourable due to their compactness, simplicity and low costs. One of the most promising methods to tailor fast saturable absorbers uses nanostructures, such as PbS nanocrystals [1] or single-wall carbon nanotubes [2, 3] embedded in various host materials. PbS nanocrystals in a silicate or a phosphate glass matrix are ideal candidates for the near-infrared region. The nanometre-sized PbS crystals or quantum dots (QD) give rise to the quantum confinement effect, which is common for semiconductor crystals of sizes comparable with the exciton Bohr radius. Enhanced quantum confinement manifests itself as a blue shift of the energy band gap and a strong nonlinearity in the range of the lowest transition, i.e. the first excitonic resonance. PbS is attractive for QD-doped glass fabrication because it has a large bulk exciton Bohr radius of 18 nm and a narrow band gap of 0.41 eV [4]. This property allows obtaining a strong quantum confinement with relatively large crystals and the absorption resonance can be tuned between 1 and 2 μm. Glasses doped with PbS nanocrystals were used as saturable absorbers for mode locking of a continuous-wave-pumped (CW-pumped) Cr:Forsterite laser [5, 6], a Yb:KYW laser [7] and a Cr^{4+}:YAG laser [8]. Further for Q-switching of an erbium–ytterbium-glass laser [9], a neodymium laser at 1.3 μm [10] and for mode locking and Q-switching of $Nd{:}KGd(WO_4)_2$ and Nd:YAG lasers [11].

Neodymium-doped vanadate crystals, such as $Nd{:}YVO_4$, $Nd{:}GdVO_4$, or mixed $Nd{:}Y_xGd_{1-x}VO_4$ crystals, are efficient laser media and have a considerable potential for diode-pumped laser systems. Their laser characteristics and their thermal properties are superior to those of Nd:YAG and, therefore, they are promising substitutes for diode-pumped Nd:YAG lasers. For example, an a-cut $Nd{:}GdVO_4$ crystal has a seven times larger absorption cross-section ($5.2 \cdot 10^{-19}$ cm^2, E||c-axis) and a three times larger emission cross-section at 1.06 μm ($7.6 \cdot 10^{-19}$ cm^2, E||c-axis)

A.A. Sirotkin · A.I. Zagumennyi · Y.D. Zavartsev · S.A. Kutovoi · V.I. Vlasov · I.A. Shcherbakov
Prokhorov General Physics Institute of the Russian Academy of Sciences, Vavilov street 38, 119991 Moscow, Russia

L. Di Labio (✉) · W. Lüthy · T. Feurer
Institute of Applied Physics, University of Bern, Sidlerstr. 5, 3012 Bern, Switzerland
e-mail: loredana.dilabio@iap.unibe.ch
Fax: +41-31-6313765

A.A. Onushchenko
S.I. Vavilov State Optical Institute, 197131 St. Petersburg, Russia

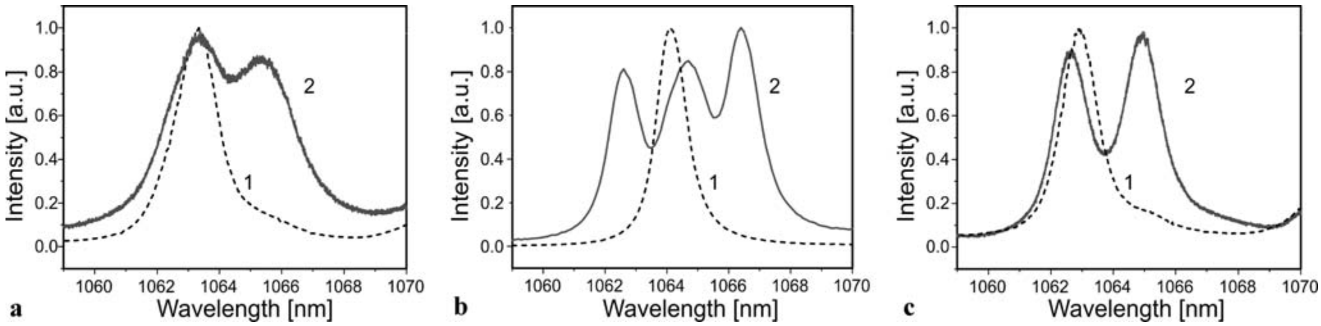

Fig. 1 Luminescence spectra around the $^4F_{3/2} \rightarrow {}^4I_{11/2}$ transition for **a** $Nd{:}Gd_{0.7}Y_{0.3}VO_4$, **b** $Nd{:}YVO_4$ and **c** $Nd{:}GdVO_4$. The *dotted curves* (*1*) refer to the a-cut and the *solid curves* (*2*) to the c-cut crystals, respectively

compared to Nd:YAG [12]. The room temperature thermal conductivity of 11.7 $W\,m^{-1}\,K^{-1}$ in the direction parallel to the c-axis for a 1.3 at.% $Nd{:}GdVO_4$ crystal exceeds the 11.1 $W\,m^{-1}\,K^{-1}$ of a 0.9 at.% Nd:YAG crystal. High-quality 0.5 at.% $Nd{:}YVO_4$ crystals even feature a thermal conductivity as high as 14.5 $W\,m^{-1}\,K^{-1}$ along the c-axis [13]. Passive mode locking has been demonstrated for an a-cut $Nd{:}GdVO_4$ laser yielding a pulse duration of 2.1 ps [14] and a Kerr-lens mode-locked a-cut $Nd{:}Gd_{0.7}Y_{0.3}VO_4$ laser produced a stable train of pulses with a minimal pulse duration of 1.7 ps at a repetition rate of 140 MHz and a maximal average output power of 630 mW [15].

Given the superior lasing characteristics of various vanadate crystals and the ideal properties of PbS nanocrystals as saturable absorbers suggests to investigate combinations of the two with respect to efficient short-pulse generation. Especially c-cut vanadate crystals have a broad emission spectrum [16] and, thus, the potential to produce short pulses. Here, we report on mode locking and Q-switching of lasers based on various c-cut Nd:vanadate crystals ($Nd{:}Gd_{0.7}Y_{0.3}VO_4$, $Nd{:}YVO_4$ and $Nd{:}GdVO_4$) by using PbS nanocrystals, Kerr lensing, or a combination of the two as saturable absorbers. The Nd^{3+} concentration in all crystals is 0.5 at.%. We demonstrate lasing in a nonselective resonator at 1065.5 nm with a c-cut $Nd{:}GdVO_4$ crystal and at 1066.4 nm with c-cut $Nd{:}YVO_4$ crystal. Q-switching and mode locking of c-cut vanadates with nanocrystalline PbS absorbers in combination with a Kerr lens have not been reported before.

2 Spectroscopic investigations of vanadate crystals

The vanadate crystals are grown by the Czochralski method on industrial installations (*Kristall-2* and *Kristall-3M*) at the A.M. Prokhorov General Physics Institute of the Russian Academy of Sciences. Optical absorption spectra of the crystals are recorded with a spectrophotometer (*Shimadzu* UV-3101PC) and the fluorescence spectra are obtained with a spectrometer based on an autocollimator tube (UV-90) and a detector (*Toshiba* TSD1304JK) under 808 nm diode laser excitation.

While the absorption spectra of a-cut (π-polarisation) and c-cut neodymium-doped vanadate crystals are almost identical, the luminescence spectra show significant differences. Figure 1 shows the normalised luminescence spectra in the wavelength range from 1059 to 1070 nm around the $^4F_{3/2} \rightarrow {}^4I_{11/2}$ transition. All c-cut vanadate crystals exhibit a considerable spectral broadening and substructures due to transitions originating from different Stark levels. For c-cut $Nd{:}Gd_{0.7}Y_{0.3}VO_4$ (Fig. 1a) and $Nd{:}GdVO_4$ (Fig. 1c) crystals the emission originates from two Stark levels, and consequently two peaks are observed. The two peaks of the $Nd{:}Gd_{0.7}Y_{0.3}VO_4$ crystals almost merge to a single emission feature centred around 1064.5 nm with a full width at half maximum (FWHM) of approximately 5.1 nm. For $Nd{:}GdVO_4$ crystals the intensity of the emission at 1065.5 nm exceeds the one at 1063.2 nm where laser oscillation in a-cut crystals is usually observed. This suggests that for a c-cut $Nd{:}GdVO_4$ crystal lasing at 1065.5 nm can be obtained even in a nonselective resonator. Figure 1b shows that the luminescence spectrum of a c-cut $Nd{:}YVO_4$ crystal consists of three transitions with the strongest line at 1066.4 nm. The three transitions cover a spectral range of almost 6 nm. For all three c-cut vanadate crystals we expect that the broader emission spectra allow for new functionalities, such as tuning, two-frequency lasing or generation of sub-picosecond pulses.

3 Tuneable lasing

The broad luminescence spectra (Fig. 1) of c-cut vanadate crystals should allow for an increased tuning range in the continuous wave mode of operation. The experimental arrangement to measure the tuning curve is shown schematically in Fig. 2.

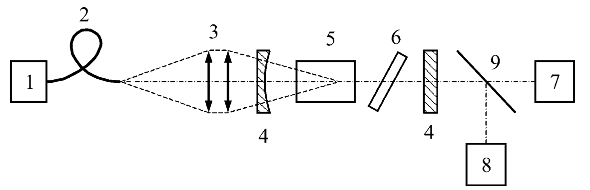

Fig. 2 Schematic arrangement of the tuneable CW Nd-doped vanadate laser. 1: pump diode, 2: fibre pigtail, 3: focusing optics, 4: laser resonator, 5: crystal, 6: intracavity Fabry–Pérot etalon, 7: powermeter, 8: spectrometer, 9: beam splitter

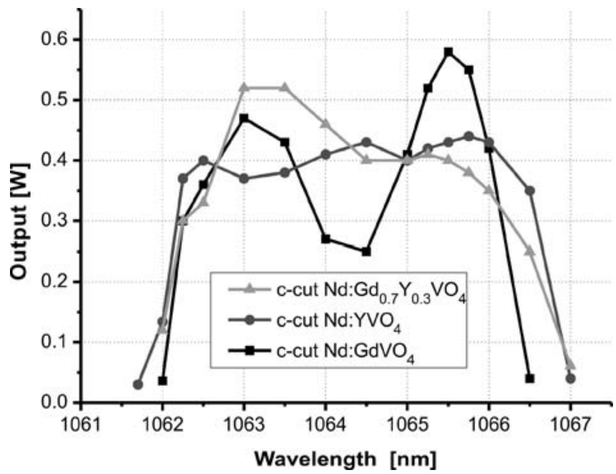

Fig. 3 The tuning curves of c-cut $Nd:Gd_{0.7}Y_{0.3}VO_4$, $Nd:YVO_4$ and $Nd:GdVO_4$ lasers

The crystal is pumped with a fibre-coupled (2) diode laser (1) at a wavelength of 808 nm (*Limo* 30-F200-DL800). Its maximum output power is 30 W in a numerical aperture of NA $= 0.22$. The output from the fibre pigtail is focused with two lenses of focal lengths $f = 20$ mm and $f = 35$ mm (3) to the active element resulting in a pump spot radius of approximately 400 μm. The size of the c-cut $Nd^{3+}:Gd_{0.7}Y_{0.3}VO_4$, $Nd:YVO_4$, and $Nd:GdVO_4$ laser crystals (5) is 4 mm × 4 mm × 6 mm and both side surfaces are antireflection (AR) coated for 1064 and 808 nm. The crystals are mounted between two water-cooled heat sinks with indium foil providing an effective and uniform thermal contact. The laser resonator consists of a spherical mirror (4) with a radius of curvature of 250 mm being highly reflective (HR) at 1064 nm and highly transmissive (HT) at 808 nm and a flat output coupler with $R = 92\%$ at 1064 nm. The overall length of the laser cavity is approximately 45 mm. Wavelength tuning is accomplished with an intracavity Fabry–Pérot etalon (6). The etalon is a 100 μm thick uncoated YAG slide.

Figure 3 shows the measured tuning curves of the three different laser crystals. All three curves very nicely reproduce the shape and structure of the corresponding luminescence spectra (see Fig. 1) and cover a spectral range between 1062 and 1067 nm. The incident pump power for the tuning experiments is 5–6 W for $Nd:YVO_4$ or $Nd:GdVO_4$ and 8 W for $Nd:Gd_{0.7}Y_{0.3}VO_4$.

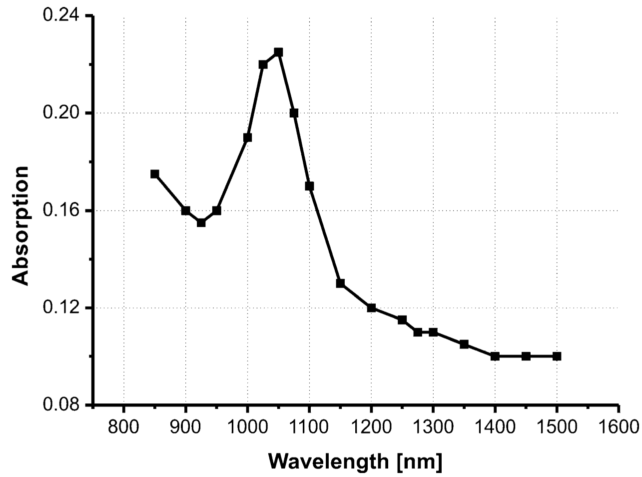

Fig. 4 Small signal absorption spectrum of a 1 mm thick PbS-doped glass slide

4 Q-switching

Passive Q-switching of $Nd:YVO_4$, $Nd:GdVO_4$ and $Nd:Gd_{0.7}Y_{0.3}VO_4$ lasers with PbS-doped glasses is demonstrated with an experimental arrangement similar to the one shown in Fig. 2, except the Fabry–Pérot etalon is replaced by a PbS-doped glass slide. The temporal duration of the Q-switched pulses is measured with a germanium avalanche photodiode (LFD-2) and recorded with an oscilloscope (*Tektronix* TDS 3052).

The PbS nanocrystals are embedded in a 1 mm thick SiO_2–Al_2O_3–NaF–Na_2O–ZnO glass matrix and the concentration is between 0.3 and 0.6 mol.%. The wavelength dependent small signal absorption spectrum is shown in Fig. 4. It features a roughly 100 nm wide peak centred at 1050 nm on top of a slowly decreasing background. From the 1 mm thick slides four wedges are prepared with a maximal thickness of 0.8, 0.6, 0.4 and 0.2 mm, respectively. Each wedge has an angle of $\sim 1.5°$ and is in direct contact to a 1 mm undoped YAG plate for cooling. With those the small signal absorption at 1064 nm can be varied continuously between 0.3 and 14%.

Passive Q-switching is obtained for all three crystal materials with pulse durations ranging from 35 to 70 ns. Pulse energies are typically on the order of 40 μJ. The best performance is found for the c-cut $Nd:Gd_{0.7}Y_{0.3}VO_4$ crystal in combination with a 14% saturable absorber. Here, the pulse duration is 35 ns and the average output power amounts to 430 mW at repetition rates of 6 to 12 kHz (pump power: 5–6 W).

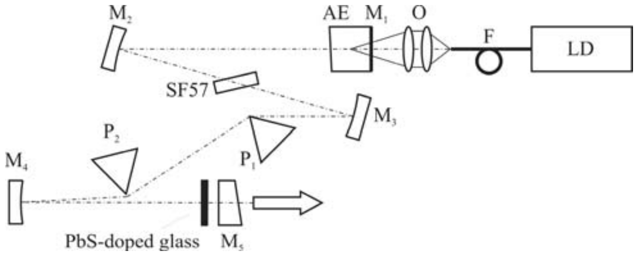

Fig. 5 Schematic of the mode-locked Nd:vanadate lasers. LD: laser diode, F: fibre pigtail, O: focusing optics, AE: active element (vanadate crystals), M_1: end mirror, M_2 and M_3: concave ($R = 100$ mm) high reflectors, SF57: Kerr-lens medium (5 mm thick), M_4: concave ($R = 250$, 150 or 100 mm) high reflector, PbS QD: saturable absorber, M_5: output coupler ($T = 4.8\%$ @ 1064 nm), P_1, P_2: prism pair (SF10)

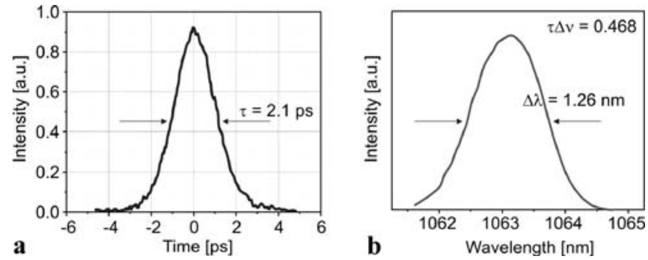

Fig. 6 **a** Intensity autocorrelation and **b** spectrum for a c-cut $Nd:Gd_{0.7}Y_{0.3}VO_4$ crystal

5 Mode locking

The experimental arrangement for mode locking is shown schematically in Fig. 5. The end mirror of the resonator is the end surface of the crystal (M_1) which has a HR coating for 1064 nm and an AR coating for 808 nm. All crystals have dimensions of 4 mm × 4 mm × 6 mm with a slightly wedged (1.5°) and AR-coated front surface to suppress etalon effects. The output coupler (M_5) is a wedge with a transmission of 4.8% at 1064 nm. The two curved folding mirrors (M_2 and M_3) with radii of 100 mm produce an additional focus at which a glass slide for Kerr lensing can be inserted. Both mirrors are tilted by ∼16° to partly compensate for aberrations. The Kerr medium is a 5 mm thick SF57 glass slide with a nonlinear refractive index of $n_2 = 4.1 \cdot 10^{-19}$ m^2/W [17] inserted at Brewster's angle. Dispersion compensation is achieved through an intracavity prism pair consisting of two SF10 prisms (P_1 and P_2). The main beam waist is located close to the output coupler and has a diameter between 20 and 100 µm with the exact value being determined by the curvature of the spherical mirror M_4 ($R = 250$, 150 or 100 mm). One of the PbS-doped glass wedges is positioned close to the output coupler M_5. Its small signal absorption can be varied from 0.3 to 6% at 1064 nm. The temporal duration of the optical pulses is measured with either a streak camera of 0.7 ps rise time (*GPI Photoelectronics Dept.* Mod. PN-01/s20) or an autocorrelator based on noncollinear second harmonic generation with a 100 µm thick BBO crystal.

Mode locking is performed with either the saturable absorber alone, the Kerr lens medium alone or a combination of the two. No mode locking could be obtained without these two elements. Due to the large beam diameter of about 300 µm inside the vanadate laser crystal, the intensity was not sufficient for self-focusing in the gain medium. Passive mode locking with PbS-doped glass alone is studied by moving the SF57 plate out of the 35 by 60 µm beam waist using it only to compensate for aberrations. Self-starting mode locking is obtained for all three crystals with the PbS-doped glass wedge (5% small signal absorption) positioned 1 to 2 mm away from the output coupler M_5. In this range the beam diameter varies from 20 to 45 µm. With a pump power of between 3 and 5 W the laser produces a stable train of pulses of duration of about 6 ps FWHM and output power of 350 mW at a pulse repetition rate of 100 MHz.

Passive mode locking with the Kerr-lens medium alone is achieved by moving the SF57 plate back to the beam waist between M_2 and M_3 and by removing the PbS saturable absorber. The long-term stability of passive mode locking with the Kerr lens depends mostly on the stability of the pump source. The duration of laser pulses measured in this regime is between 2 and 4 ps with an average power of 240 mW (pump power: 5 W).

Laser performance is most stable and produces the shortest laser pulses when a hybrid passive mode-locking scheme is used which is based on a combination of the PbS saturable absorber and the Kerr-lens medium. For the c-cut $Nd:Gd_{0.7}Y_{0.3}VO_4$ crystal the shortest measured autocorrelation trace has a FWHM of 2.1 ps. Assuming a $sech^2$ intensity profile, the pulse duration is on the order of 1.4 ps. For a pump power of 6 W the average output power is measured to be 255 mW, and the repetition rate is 100 MHz. Figure 6 shows a typical intensity autocorrelation trace and the corresponding optical spectrum with a bandwidth of 1.26 nm FWHM. The resulting time-bandwidth product is $\tau\Delta\nu = 0.468$, somewhat larger than the transform limit of $\tau\Delta\nu = 0.32$.

6 Conclusions

C-cut $Nd:Gd_{0.7}Y_{0.3}VO_4$, $Nd:YVO_4$, and $Nd:GdVO_4$ crystals show an amplification bandwidth that is much broader than that of the corresponding a-cut crystals, roughly ranging from 1062 to 1067 nm. Consequently, the tuning range of continuous wave lasers is shown to be considerably wider. The specific shape of the luminescence spectra allows for lasing in a nonselective resonator at 1065.5 nm with $Nd:GdVO_4$ and at 1066.4 nm with $Nd:YVO_4$. When these crystals are combined with a PbS-doped glass Q-switching produces pulses between 35 and 70 ns. Specifically, the c-cut

$Nd{:}Gd_{0.7}Y_{0.3}VO_4$ crystal yields 35 ns long pulses with an average output power of 430 mW at a repetition rate of 6–12 kHz at a pump power of 5–6 W. In a resonator suitable for mode locking the PbS-doped saturable absorber generates a stable train of pulses with a repetition rate of 100 MHz. At a pump power of 5 W the individual pulses are 6 ps long and the average output power is 255 mW. By combining the PbS-doped absorber with Kerr lens pulses as short as 1.4 ps are measured. This pulse duration is still larger than the bandwidth limit and we expect that even shorter pulses can be obtained by further optimising the PbS-doped glass.

Acknowledgements This work was supported in part by the Swiss National Science Foundation under contract IB7420-110873/1.

References

1. A.A. Onushchenko, A.A. Zhilin, G.T. Petrovskiĭ, É.L. Raaben, M.S. Gaponenko, A.M. Malyarevich, K.V. Yumashev, V.V. Golubkov, J. Opt. Technol. **73**(9), 576 (2006)
2. N.N. Il'ichev, E.D. Obraztsova, S.V. Garnov, S.E. Mosaleva, Quantum Electron. **34**(6), 572 (2004)
3. N.N. Il'ichev, E.D. Obraztsova, P.P. Pashinin, V.I. Konov, S.V. Garnov, Quantum Electron. **34**(9), 785 (2004)
4. I. Kang, F.W. Wise, J. Opt. Soc. Am. B **14**(7), 1632 (1997)
5. P.T. Guerreiro, S. Ten, N.F. Borrelli, J. Butty, G.E. Jabbour, N. Peyghambarian, Appl. Phys. Lett. **71**(12), 1595 (1997)
6. K. Wundke, S. Pötting, J. Auxier, A. Schülzgen, N. Peyghambarian, N.F. Borrelli, Appl. Phys. Lett. **76**(1), 10 (2000)
7. A.A. Lagatsky, A.M. Malyarevich, V.G. Savitski, M.S. Gaponenko, K.V. Yumashev, A.A. Zhilin, C.T.A. Brown, W. Sibbett, IEEE Photon. Technol. Lett. **18**(1), 259 (2006)
8. A.A. Lagatsky, C.G. Leburn, C.T.A. Brown, W. Sibbett, A.M. Malyarevich, V.G. Savitski, K.V. Yumashev, E.L. Raaben, A.A. Zhilin, Opt. Commun. **241**, 449 (2004)
9. J.F. Philipps, T. Töpfer, H. Ebendorff-Heidepriem, D. Ehrt, R. Sauerbrey, N.F. Borrelli, Appl. Phys. B **72**(2), 175 (2001)
10. V.G. Savitski, A.M. Malyarevich, K.V. Yumashev, V.L. Kalashnikov, B.D. Sinclair, H. Raaben, A.A. Zhilin, Appl. Phys. B **79**(3), 315 (2004)
11. A.M. Malyarevich, V.G. Savitski, P.V. Prokoshin, N.N. Posnov, K.V. Yumashev, E. Raaben, A.A. Zhilin, J. Opt. Soc. Am. B **19**(1), 28 (2002)
12. T. Jensen, V.G. Ostroumov, J.-P. Meyn, G. Huber, A.I. Zagumennyi, I.A. Shcherbakov, Appl. Phys. B **58**(5), 373 (1994)
13. A.I. Zagumennyi, P.A. Popov, F. Zerouk, Yu.D. Zavartsev, S.A. Kutovoi, I.A. Shcherbakov, Quantum Electron. **38**(3), 227 (2008)
14. E. Sorokin, I. Sorokina, E. Winter, A.I. Zagumennyi, I.A. Shcherbakov, OSA Proc. Adv. Solid-State Lasers **15**, 238 (1993)
15. A.A. Sirotkin, S.A. Kutovoi, Yu.D. Zavartsev, V.A. Mikhailov, A.I. Zagumennyi, Yu.L. Kalachev, I.A. Shcherbakov, R. Renner-Erny, W. Lüthy, T. Feurer, Laser Phys. Lett. **4**(9), 652 (2007)
16. V.I. Vlasov, S.V. Garnov, Yu.D. Zavartsev, A.I. Zagumennyi, S.A. Kutovoi, A.A. Sirotkin, I.A. Shcherbakov, Quantum Electron. **37**(10), 938 (2007)
17. S.R. Friberg, P.W. Smith, IEEE J. Quantum Electron. **QE-23**(12), 2089 (1987)